

Neutron Irradiation Damage Analysis on Single and Dual Layer 150nm CMOS SPADs



UNIVERSITÀ
DI PAVIA

Fatemeh Shojaei, Joana Minga, Lodovico Ratti,
Gianmarco Torilla, Carla Vacchi

University of Pavia and INFN, Pavia, Italy



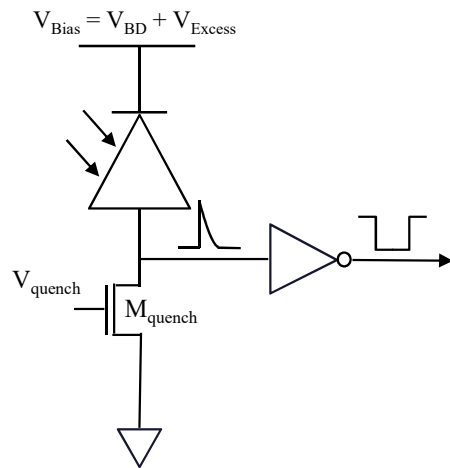
RADOPT 2023: Workshop on Radiation Effects on
Optoelectronic Detectors and Photonics Technologies

Toulouse, France
Nov. 28-Dec. 1, 2023

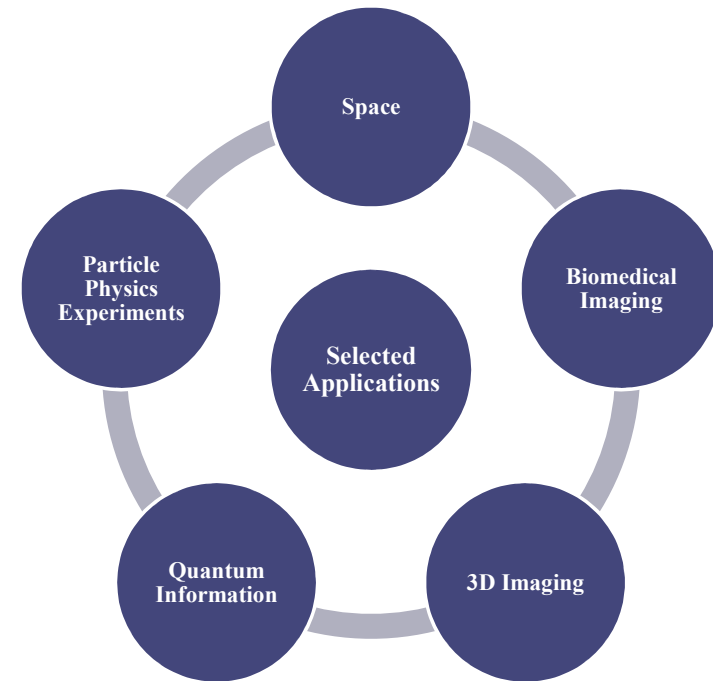
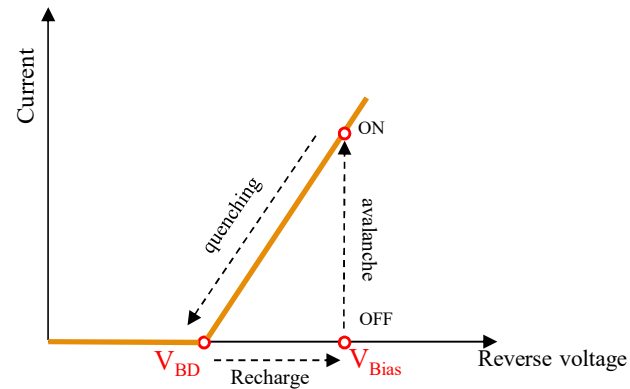
SPAD Working Principle and Applications

- **Single Photon Avalanche Diode (SPAD)** internal high gain \Rightarrow **high timing resolution**
- **CMOS compatibility** \Rightarrow enable large array fabrication with **integrated front-end electronics** \Rightarrow **cost-effective**

Quenching circuit



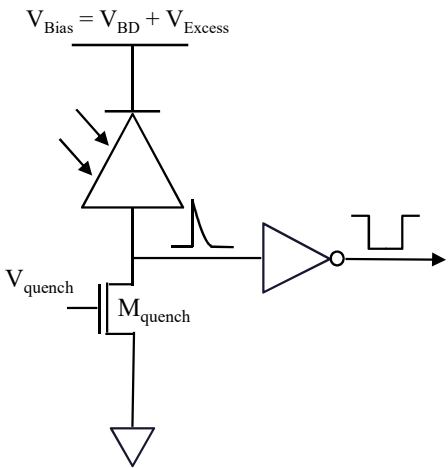
Dynamic behavior of a SPAD.



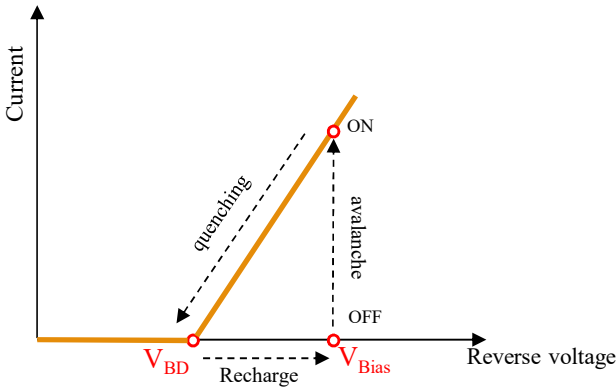
SPAD Working Principle and Applications

- **Single Photon Avalanche Diode (SPAD)** internal high gain ➡ **high timing resolution**
- **CMOS compatibility** ➡ enable large array fabrication with **integrated front-end electronics** ➡ **cost-effective**

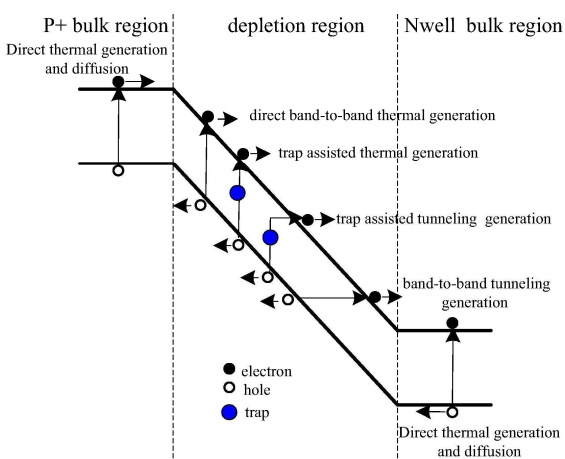
Quenching circuit



Dynamic behavior of a SPAD.

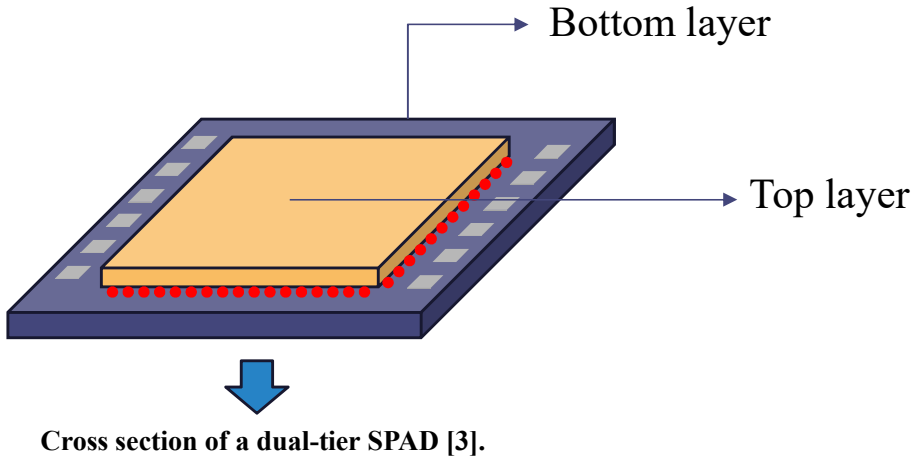
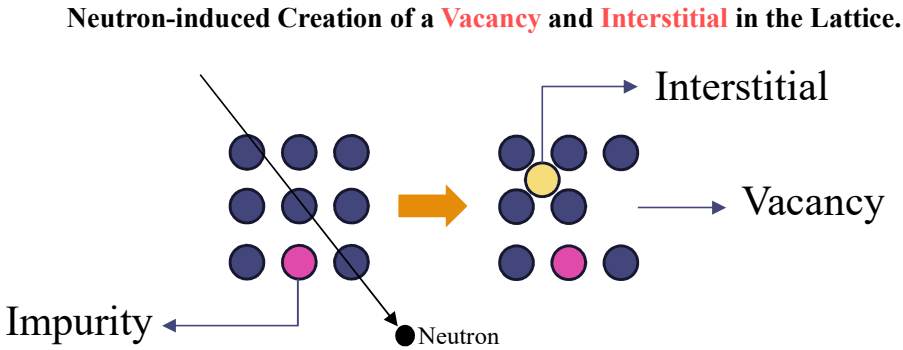


Carrier generation mechanisms [1]

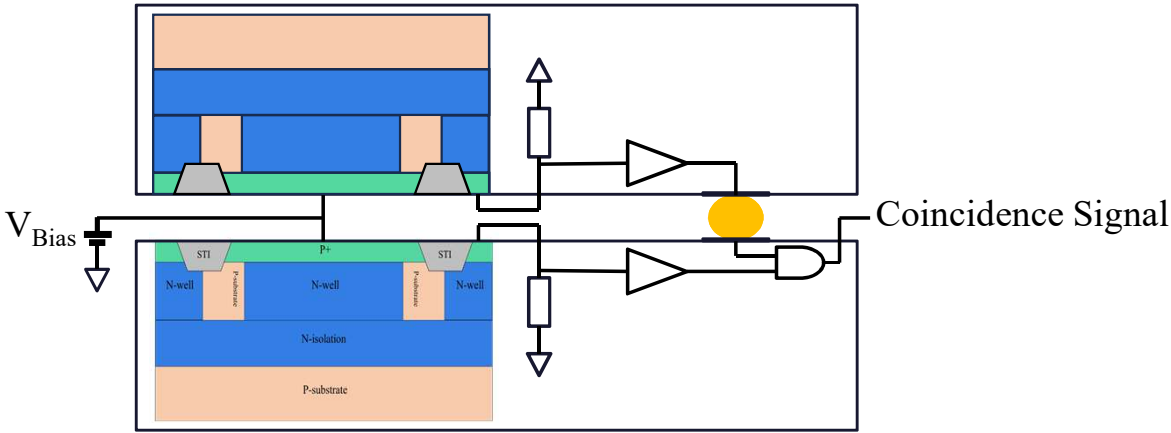
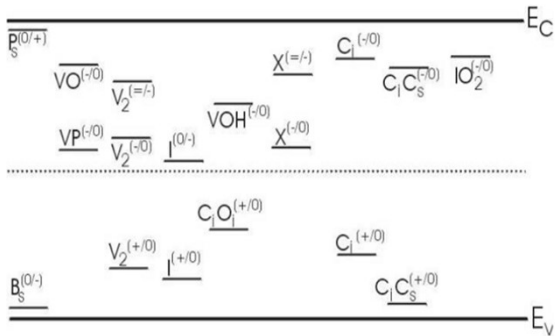


[1] Xu Y., Xiang P., Xie X., Solid-State Electronics, vol. 129, 2017, pp. 168-174.

Neutron damage and dual-layer configuration



Energy levels of radiation-induced defects within the silicon bandgap [2].



$$DCR_{\text{coincidence}} = 2 \times \Delta t \times DCR_b \times DCR_t$$

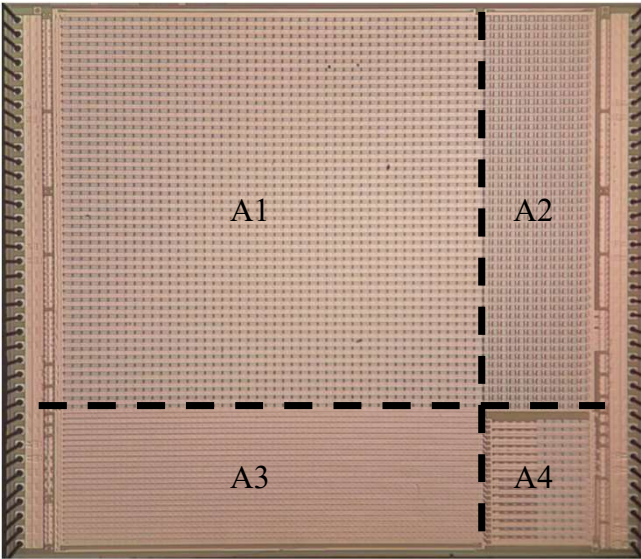
[2] Lee S. J., *SciPost Phys. Proc.*, vol. 12, no. 030, Jul. 2023
 [3] L. Ratti, P. Brogi, G. Collazuol, et al., *Front. Phys.*, vol. 8, p. 607319 2021

DESCRIPTION OF DEVICES UNDER TEST (DUTS) AND IRRADIATION CAMPAIGN

DUTS Description

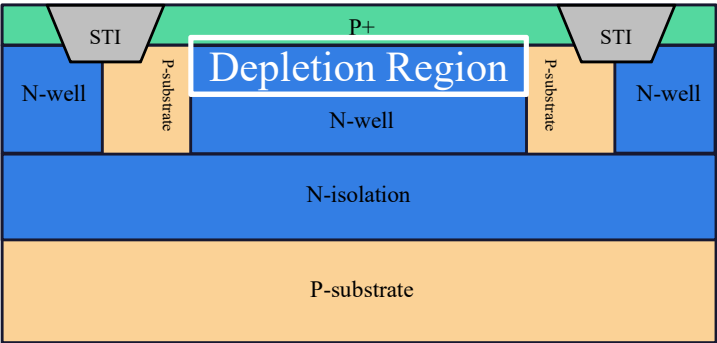
- Three chips fabricated in **150nm CMOS Technology**:
 - Two single-layer (F2 and S2)
 - One dual-layer (D1)

Microphotograph of a single layer chip.



• The focus of this study is **A1** and **A3**

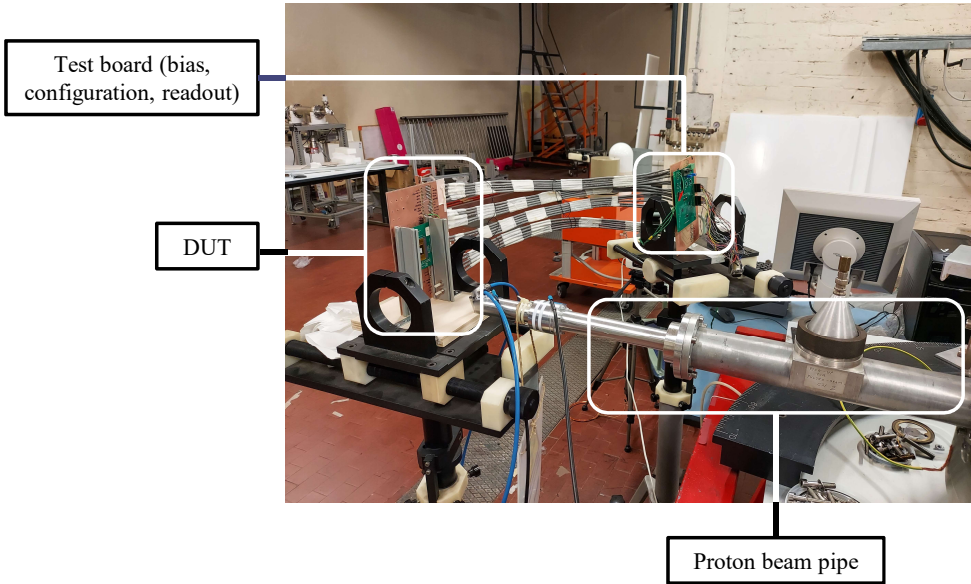
array	# of cells	pixel pitch (μm)	fill factor	active area (μm ²)
A1	2304	75	66%	70 × 52
A2	576	75	44%	47 × 57
A3	1728	50	39%	44 × 24
A4	165	75	52%	44 × 24



Simplified cross section of a SPAD layout employed in arrays A1 and A3.

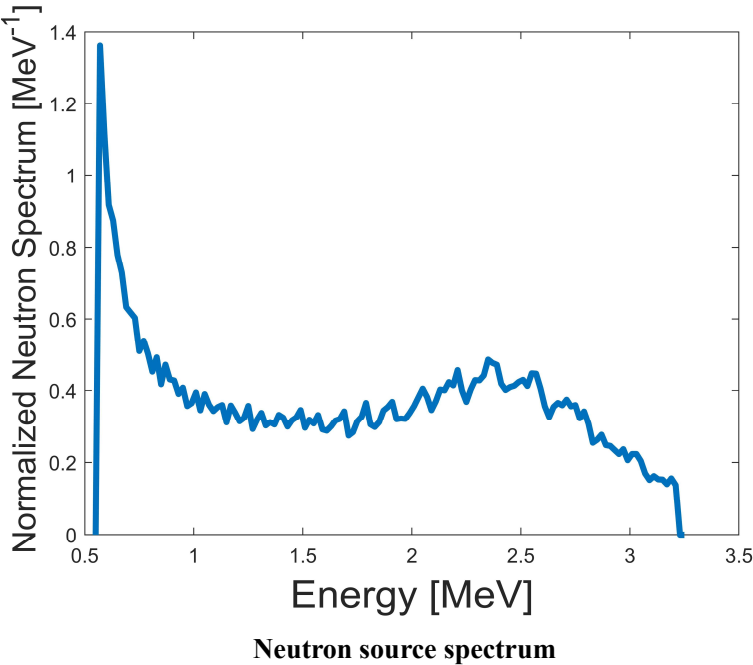
Irradiation Campaign

- The radiation source generates steady stream of neutrons by bombarding a **beryllium target** with **mono-energetic protons (5 MeV)**.
- Proton current fluctuations is considered in neutron fluence calculations
- DUTs are positioned **4.5 cm** away from the neutron source.
- The neutron flux varies linearly with the proton current.



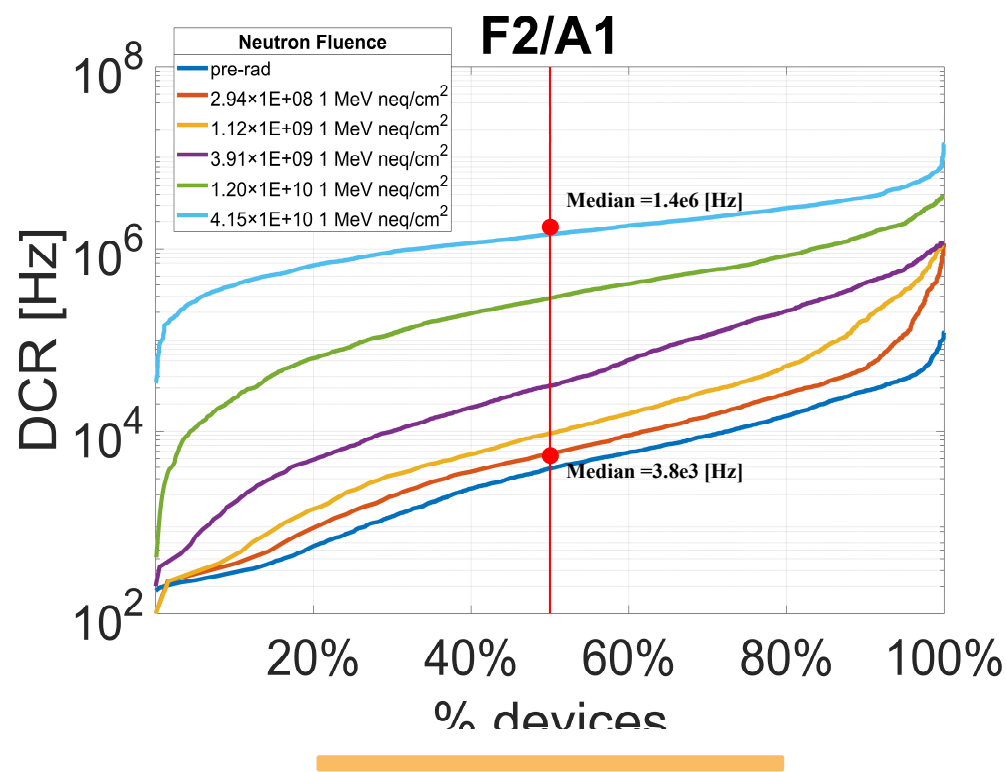
Irradiation Steps

Chip Type	No. of Steps	Fluences at the end of each step (1 MeV neutron equivalent cm ⁻²)
F2	5	2.94×10 ⁸ , 1.12×10 ⁹ , 3.91×10 ⁹ , 1.20×10 ¹⁰ , 4.15×10 ¹⁰
S2	3	2.92×10 ⁸ , 1.13×10 ⁹ , 3.90×10 ⁹
D1	3	2.92×10 ⁸ , 4.09×10 ⁹ , 4.29×10 ¹⁰

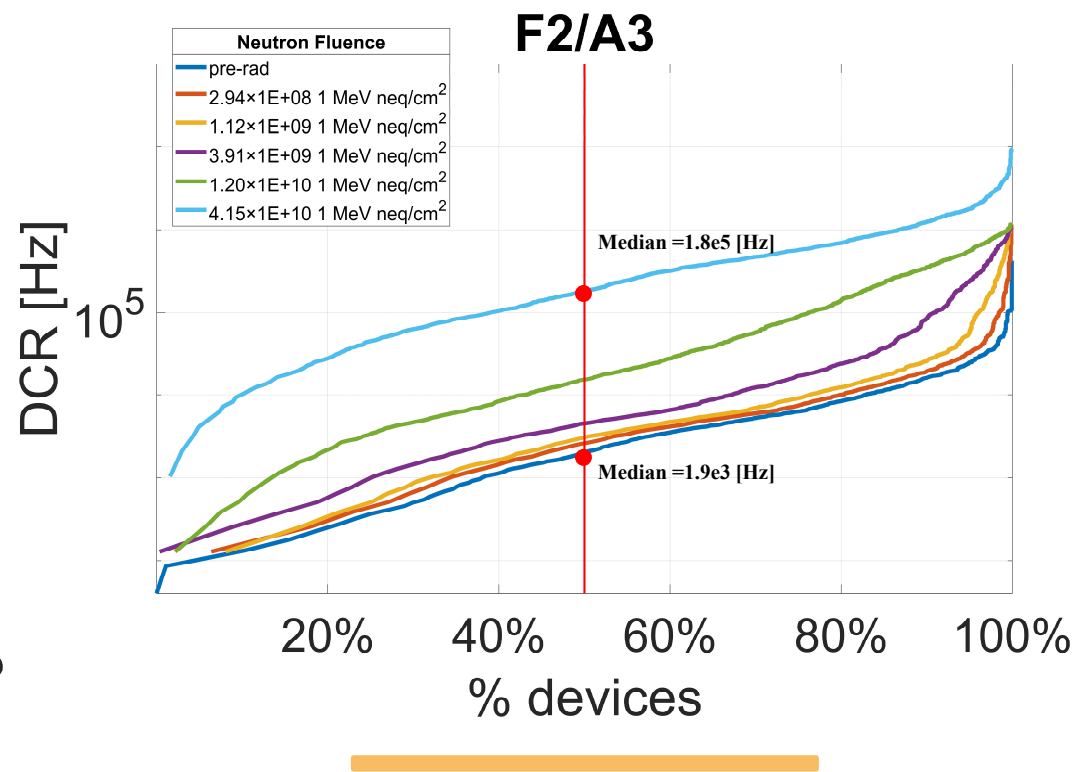


DCR MEASUREMENTS AND DCR INCREASE MODELING

Fluence-Dependent DCR Measurements: Single-Layer

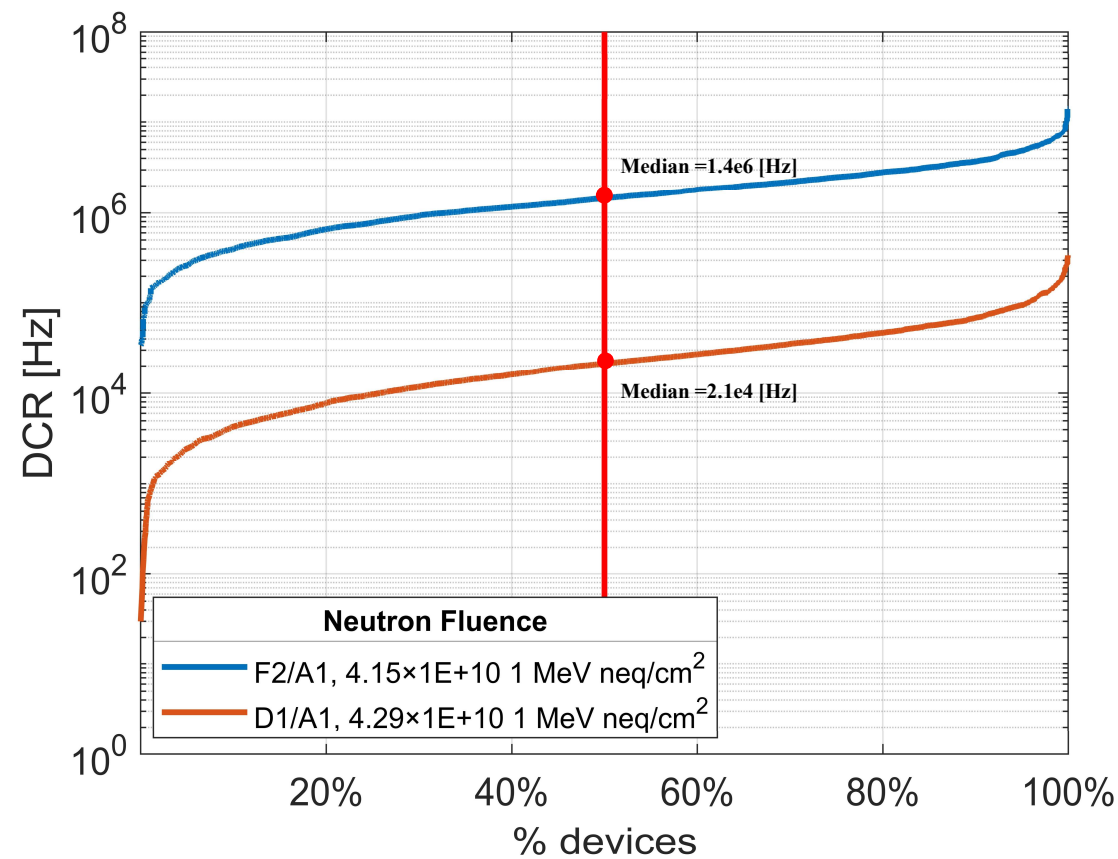


Cumulative DCR curves for chip F2, array A1 before and after 5 ascending irradiation fluences.

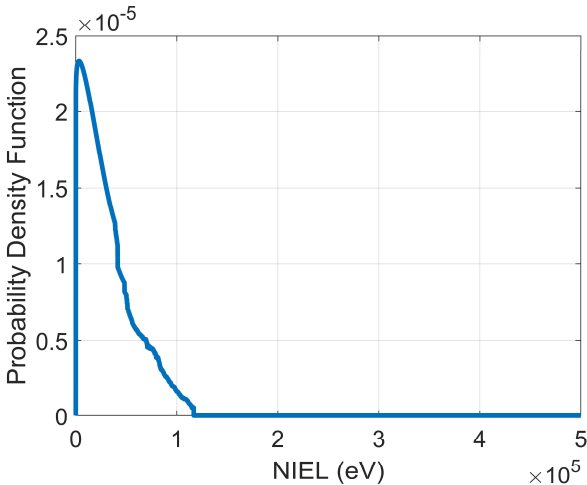
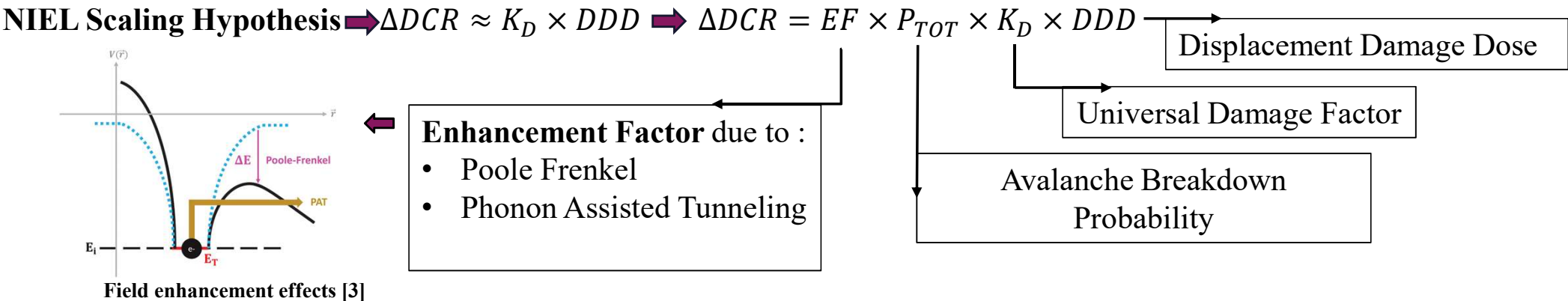


Cumulative DCR curves for chip F2, array A3 before and after 5 ascending irradiation fluences.

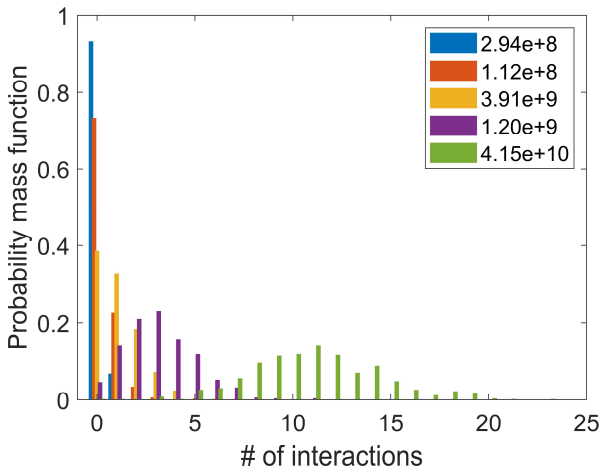
DCR Measurements: Single and Dual-layer Comparison



Cumulative DCR curves comparison for both array A1 embedded in chips F2 and D1 after exposure to similar fluences.



Normalized PDF for the NIEL released in the SPAD depletion region



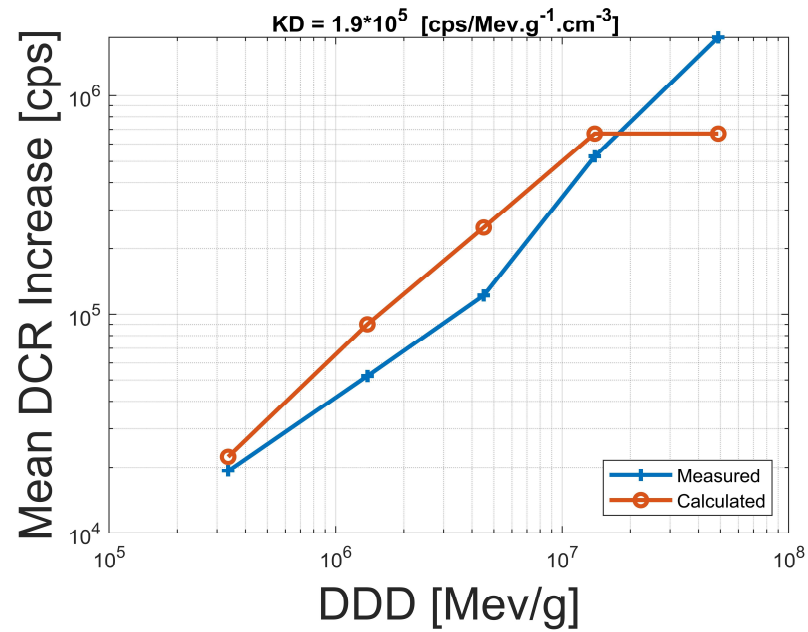
PMF of interactions in F2/A1 SPADs at varying fluences within the depletion region

- A model [4] including **Lindhard partition function** is used to estimate **non-ionizing energy** dissipated by a **single neutron**, considering energy spectrum of the source:

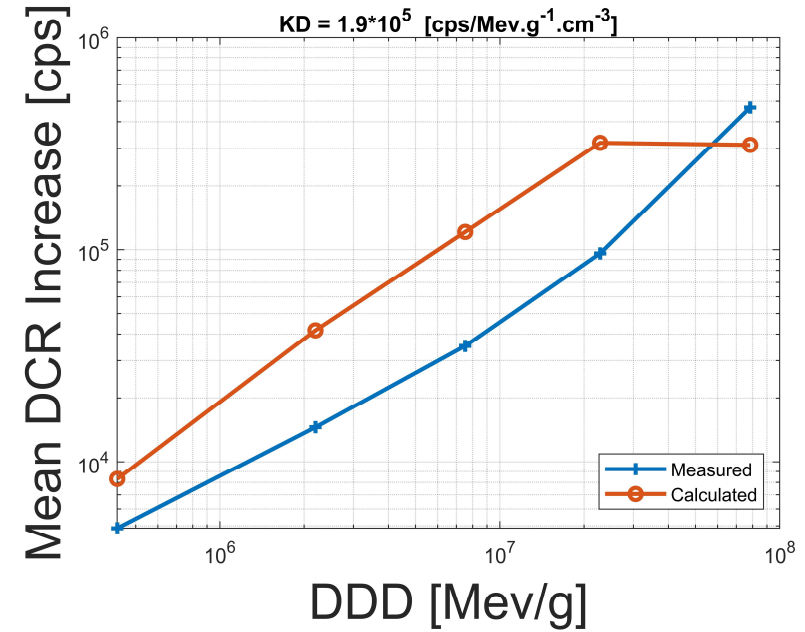
$$T_d = h(T) = \begin{cases} 0, & T < E_d \\ \frac{T}{1 + F_L \left[a \left(\frac{T}{E_L} \right)^{\frac{1}{6}} + b \left(\frac{T}{E_L} \right)^{\frac{3}{4}} + \left(\frac{T}{E_L} \right) \right]}, & T \geq E_d \end{cases}$$
- By employing $Pd \approx \Sigma(E_{inp})(z_2 - z_1)$ and **Monte Carlo simulations**, the probability mass function of the number of interactions at varying neutron fluences can be estimated.

DCR Increase modeling results

- In this modeling approach, the effect of annealing is also taken into account.



Mean DCR Increase Vs DDD for F2/A1 pixels

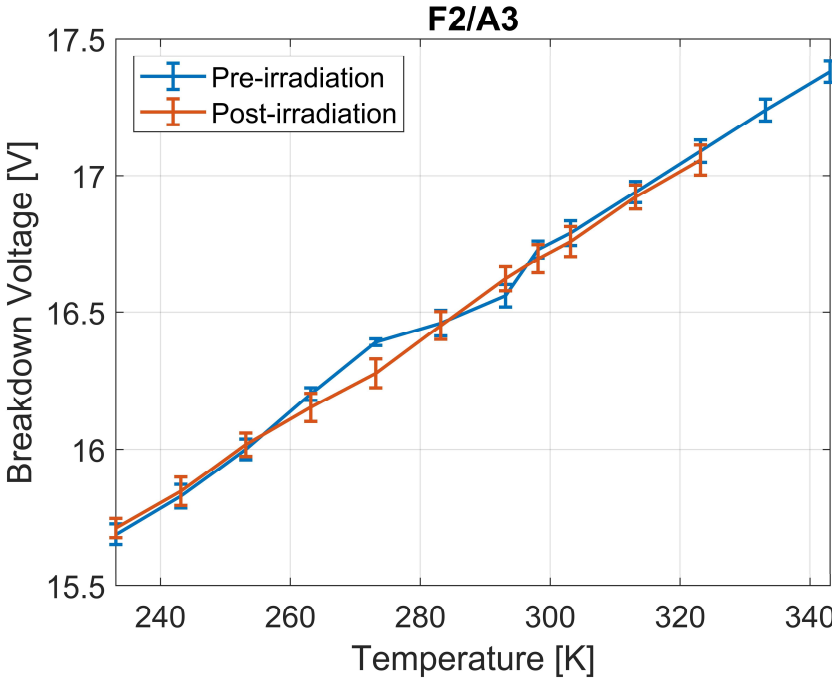
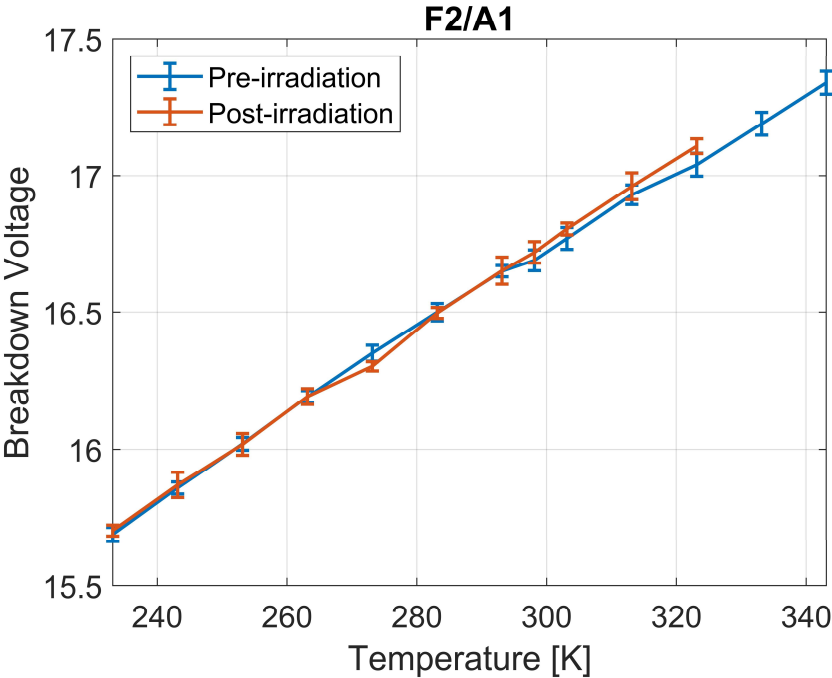


Mean DCR Increase Vs DDD for F2/A3 pixels

TEMPERATURE-DEPENDENT MEASUREMENTS

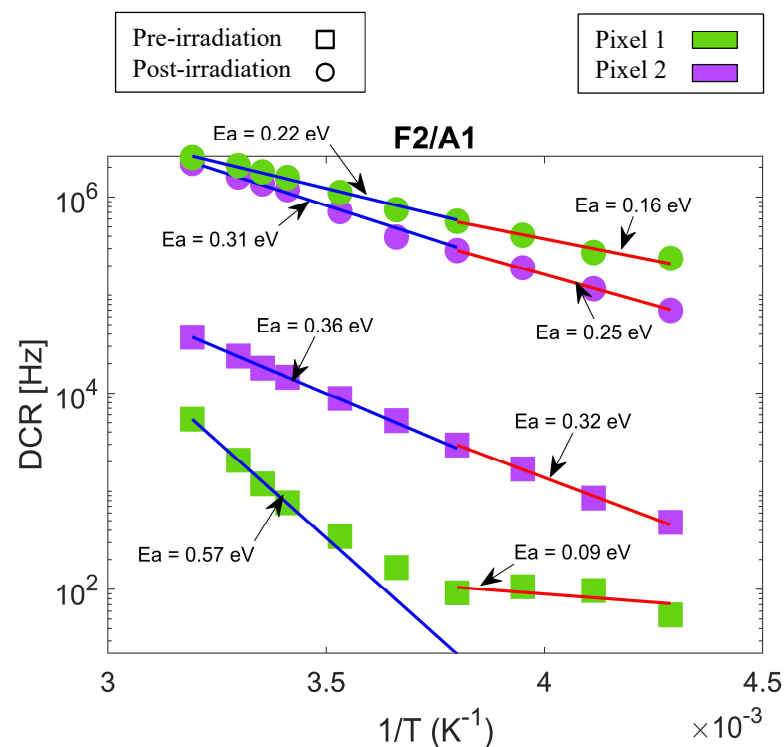
Breakdown voltage Vs temperature

- Breakdown voltage increases with temperature.
- No visible degradation occurs in breakdown voltage after irradiation.



Arrhenius plots

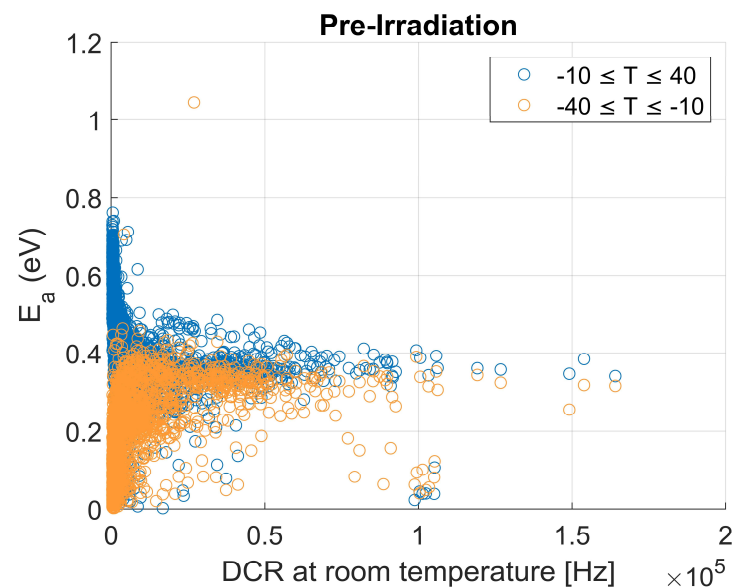
- Arrhenius Equation $\Rightarrow DCR = Ae^{-\frac{E_a}{k_B T}}$



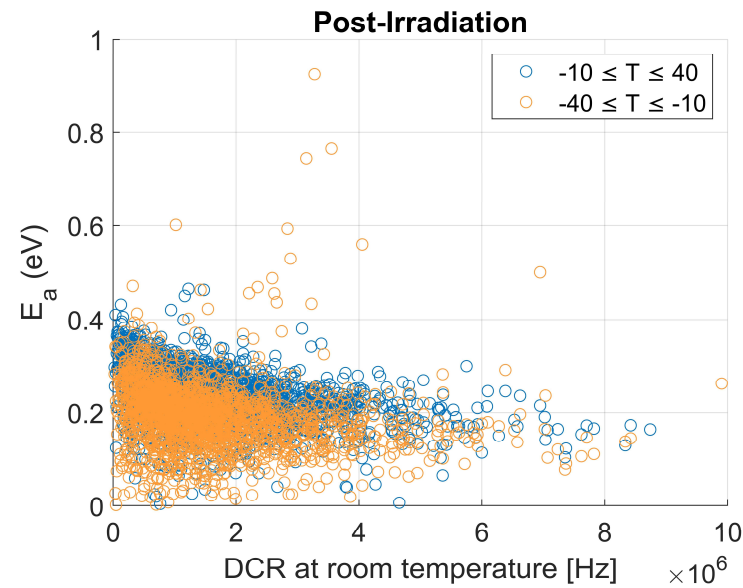
Arrhenius plots for two representative pixels: before and after radiation

- Pre-irradiation
- Low temperatures:
 - activation energy close to zero \Rightarrow Band to Band Tunneling (BTBT)
 - activation energy close to silicon midgap energy ($\frac{E_g}{2}$) \Rightarrow Shockley-Read-Hall (SRH) & Trap Assisted Tunneling (TAT)
- High temperatures:
 - activation energies close to, but higher than $\frac{E_g}{2}$ \Rightarrow SRH
 - activation energies close to, but lower than $\frac{E_g}{2}$ \Rightarrow SRH & TAT (the lower E_a, the greater the contribution of TAT)
- Post-irradiation
- high and low temperatures:
 - Low and high-temperature E_a are close to each other \Rightarrow TAT as the dominant generation mechanism.

Neutron damage effect on E_a distribution



Activation energy distribution versus DCR for F2A1 at room temperature before radiation



Activation energy distribution versus DCR for F2A1 at room temperature after radiation

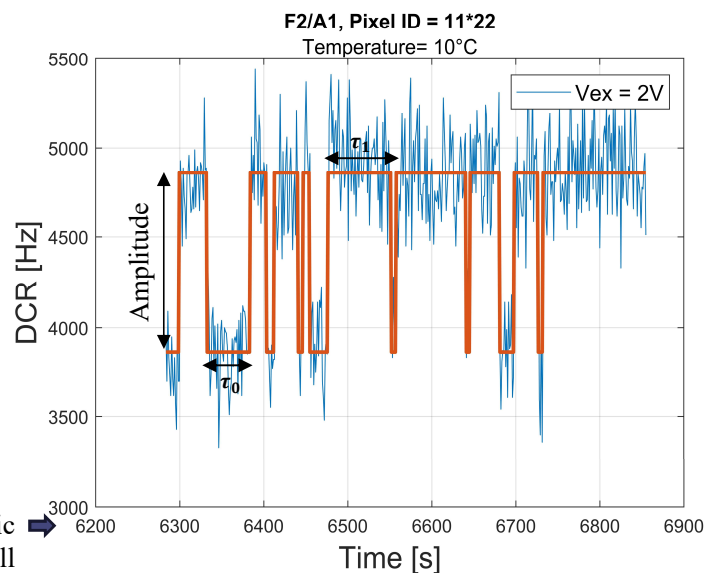
Mean Activation Energies for F2

Array	T Range	Mean E_a [eV] pre-rad	Mean E_a [eV] post-rad
A1	$-10 \leq T \leq 40$	0.4191	0.2425
	$-40 \leq T \leq -10$	0.22	0.1936
A3	$-10 \leq T \leq 40$	0.3959	0.2821
	$-40 \leq T \leq -10$	0.2118	0.2309

RANDOM TELEGRAPH SIGNAL NOISE (RTSN)

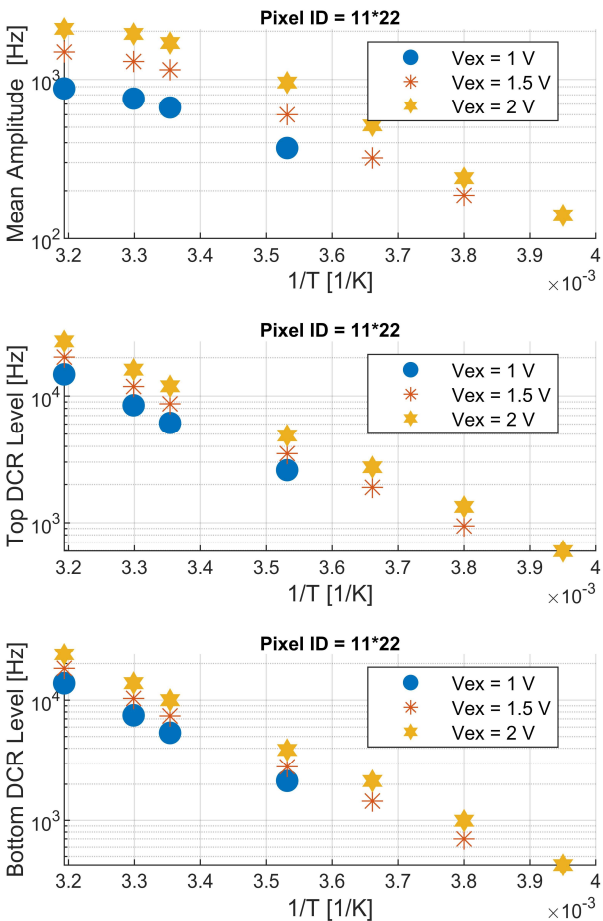
RTS: BEFORE IRRADIATION

- **Random Telegraph Signal Noise (RTSN):** random fluctuations between two or more discrete levels in DCR.
- The exact origin of this phenomenon is not fully understood.
 - Potential Causes [4]:
 - Change in di-vacancy or multi-vacancy states
 - Inter-center charge transfer between close defects
 - Metastable defects
 - P-V complex



Detailed zoom-in on a specific segment within the overall nearly 3h time window.

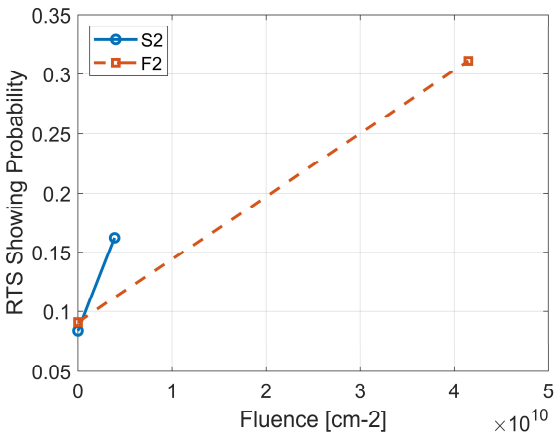
Time-resolved DCR, before irradiation.



Two-level RTS features Vs $\frac{1}{T}$, before irradiation.

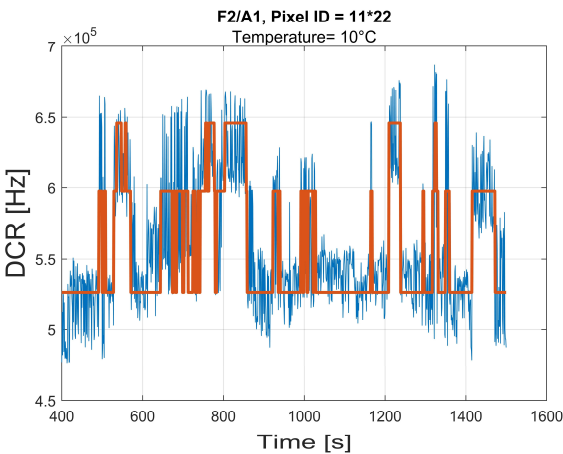
RTS: after irradiation

- Neutron damage increases the number of pixels showing RTS behavior.

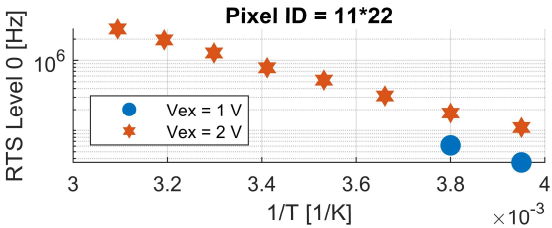
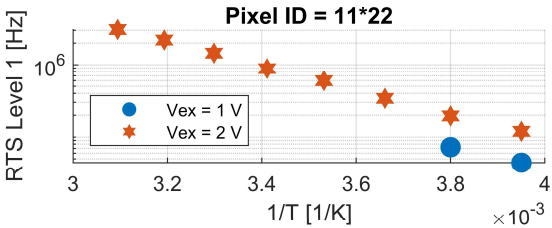
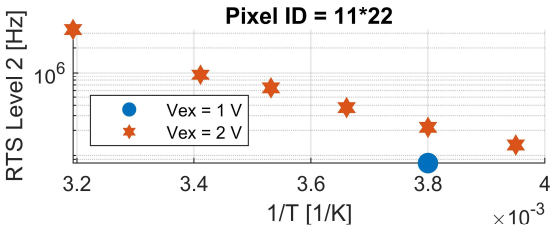
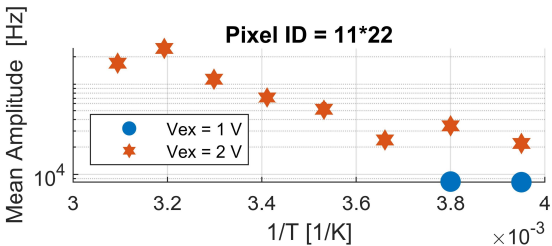


RTS showing probability Vs neutron fluence

- Number of RTS levels increased after irradiation.



Time-resolved DCR, after irradiation.



Three-level RTS features Vs $\frac{1}{T}$, after irradiation.

- **The investigation into the effects of neutron damage on CMOS SPADs has yielded the following results:**
 - **DCR increases** notably, characterized by a **widespread DCR distribution**. This increase exhibits a **linear dependency** on the DDD and developed models align well with these observations.
 - The adoption of a **dual configuration** improves the radiation tolerance, achieving a reduction in the DCR by about **two orders of magnitude** compared to a single SPAD layer following exposure to a fluence of nearly 4.20×10^{10} 1 MeV neutron equivalent cm^{-2} .
 - While neutron damage leads to a **decrease in activation energies** due to an increase in TAT generation, breakdown voltage remains unaffected.
 - There is a significant increase in the **number of pixels exhibiting RTS**, alongside a rise in the **number of levels within the RTS**.
- **What to do next:**
 - Characterizing bulk and TID effects in 110nm CMOS SPADs in terms of DCR, afterpulsing, Photon Detection Probability (PDP), timing jitter, and crosstalk.
 - Identify the specific defects responsible for RTS by analyzing activation energies extracted from time constants.

**THANK YOU FOR YOUR
ATTENTION**

